

1 **Development of Localized Surface Plasmon Resonance biosensors for the detection of**  
2 ***Brettanomyces bruxellensis* in wine**

3

4 Marisa Manzano\*<sup>1</sup>, Priya Vizzini<sup>1</sup>, Kun Jia<sup>2,3</sup>, Pierre-Michel Adam<sup>2</sup>, Rodica Elena Ionescu<sup>2\*</sup>

5

6 <sup>1</sup>Department of Food Science, University of Udine, via Sondrio 2/A, 33100 Udine, Italy

7

8 <sup>2</sup>Laboratoire de Nanotechnologie et d'Instrumentation Optique, Institute Charles Delaunay,

9 Universite' de technologie de Troyes, UMR CNRS 6281, 12 Rue Marie-Curie CS 42060,

10 10004 Troyes Cedex, France

11 <sup>3</sup>School of Microelectronics and Solid-State Electronics, University of Electronic Science and

12 Technology of China, 610054 Chengdu, China (*present address*)

13

14

15 \*corresponding authors:

16 Marisa Manzano<sup>1,\*</sup>, Department of Food Science, via Sondrio 2/A, 33100 Udine, Italy, tel:

17 +390432558127, Fax: +390432558130

E-mail: [marisa.manzano@uniud.it](mailto:marisa.manzano@uniud.it)

18 Rodica Elena Ionescu<sup>2,\*</sup>, Laboratoire de Nanotechnologie et d'Instrumentation Optique,

19 Institute Charles Delaunay, Universite' de technologie de Troyes, UMR-CNRS 6281, 12 Rue

20 Marie-Curie CS 42060, 10004 Troyes Cedex, France,

21 tel: (33) 3 25 75 97 28; fax: (33) 3 25 71 84 56

22 E-mail: [elena\\_rodica.ionescu@utt.fr](mailto:elena_rodica.ionescu@utt.fr)

23 **Abstract**

24 Incident light interacting with noble-metal nanoparticles with smaller sizes than the wavelength of  
25 the incident light induces Localised Surface Plasmon Resonance (LSPR). In this work a gold  
26 nanostructured surface was used for the immobilization of a 5' end Thiol modified DNA probe to  
27 develop a LSPR nanobiosensor for the detection of the spoiler wine yeast *Brettanomyces*  
28 *bruxellensis*. Gold was evaporated to obtain a gold thickness of 4 nm. 2  $\mu$ L of the DNA from the  
29 target microorganism and the negative control at various concentrations were used to test the  
30 specificity and sensitivity of the LSPR technique. Changes in the optical properties of the  
31 nanoparticles due to DNA-probe binding are reflected in the shift of LSPR extinction maximum ( $\lambda$   
32  $_{max}$ ). The results obtained using as target microorganism *B. bruxellensis*, and as negative control *S.*  
33 *cerevisiae* demonstrated the specificity of both the DNA-probe and the protocol. The LSPR  
34 spectrophotometry technique detect 0.01 ng/ $\mu$ L DNA target confirming the possibility to utilise this  
35 system for the detection of pathogen microorganisms present in low amount in food and beverage  
36 samples.

37

38 **Keywords:** Localized Surface Plasmon Resonance (LSPR), *Brettanomyces bruxellensis*,  
39 genosensor, Scanning Electron Microscopy

40

41

## 42 **1. Introduction**

43 In the last decade the optical properties of noble metal nanoparticles that exhibit unique extinction  
44 spectra induced various authors to explore alternative strategies for the development of optical  
45 biosensors. The interaction between metals and biomolecules opened a wide field of applications  
46 for biosensors, from ecology, to medicine and food analysis. Moreover, optical properties of gold  
47 nanostructures, which show high chemical stability, allowed the utilization of Localized Surface  
48 Plasmon Resonance (LSPR) for the construction of sensitive biosensors [1].

49 LSPR biosensors, analogously to SPR sensors, based on LSPR spectroscopy, transducing small  
50 changes in the refractive index near a nanoscale noble metal surface into a measurable wavelength  
51 shift [2, 3]. LSPR is a collective oscillation of the conduction band electrons at the nanoparticles'  
52 surface that develops when incident electromagnetic radiation is of appropriate frequency. The  
53 properties of the particles (i.e. size, shape and dielectric function) influence the plasmonic  
54 oscillation that occurs at a specific resonance wavelengths [4]. The possibility to change these  
55 parameters allows the application on various fields such as DNA detection. Biological molecules  
56 can be detected as their presence induces a modification of refractive index near the metal surface.  
57 All conditions and parameters have to be optimized to obtain repeatability and sensitivity of the  
58 LSPR biosensors. Metal nanoparticles size, shape, interparticle separation, and metal nanoparticle  
59 fabrication parameters (time, temperature, thickness of metal deposition layer, etc.) are important  
60 points to optimize for the obtained specificity and sensitivity. Thus the homogeneity of the  
61 nanoparticles has to be evaluated, mostly by using a Scanning Electron Microscope (SEM).

62 One important characteristic of the LSPR biosensors is the high sensitivity that they can reach due  
63 to the interaction of the biomolecules with highly localized fields, one application being the  
64 detection of DNA. As demonstrated by Spadavecchia et al. [5] using labelling strategies such as the  
65 utilization of gold nanorods (AuNRs) and gold nanostars (AuNSs) the LSPR biosensor reach a high  
66 sensitivity.

67 One other characteristic of these biosensors is that they can be useful for high throughput  
68 monitoring both in proteomics and DNA research [6] promising screening platforms in a highly  
69 minaturized format that requires small volumes of analyte solutions [7, 10]. The common way to  
70 detect microorganisms present in samples using DNA as target is based on the utilization of one  
71 labeled DNA molecules, mostly by fluorescent tags, to increase sensitivity.

72 Common methods based on ELISA assays, and PCR using the specific hybridization of the target  
73 DNA to one or two specific probes, while when biosensors use the amplicon as a target, the  
74 amplification step cause a delay in the achievement of the results [8].

75 The aim of this work was the development of LSPR nanobiosensors for the rapid and sensitive  
76 detection of *Brettanomyces bruxellensis*, a spoiler yeast worldwide well-known to produce  
77 unpleasant aromas in wine. As Au NPs have been the system-of-choice in preparation of LSPR  
78 biosensors, a gold nanostructured surface was prepared and used for the immobilization of either a  
79 specific or non-specific DNA probe used as receptor for the target DNA molecule extracted from  
80 wine yeasts.

81

## 82 **2. Materials and methods**

### 83 *2.1 Materials and equipment*

84 The reagents utilised for the preparation of the buffer solutions listed below were acquired from  
85 Sigma–Aldrich (Switzerland). Three buffers: 1X PBS (10X, NaCl 1.5 M, Na<sub>2</sub>HPO<sub>4</sub> anhydrous 81  
86 mM, NaH<sub>2</sub>PO<sub>4</sub> anhydrous 19 mM); 1X SSPE (20X: NaCl 3M, NaH<sub>2</sub>PO<sub>4</sub> anhydrous 230 mM,  
87 EDTA x 2H<sub>2</sub>O 25 mM and 1X TRIS-HCl (10X, Tris-HCl 0.5 M) were compared for their  
88 contribution over the biofunctionalization steps of the gold nanostructured surfaces. A complex  
89 made using the Thiol capture probe at 100 ng/μL and DNA from the target yeasts at 10 ng/μL were  
90 used to select the buffer for the hybridisations.

91 All LSPR measurements were obtained by using a home-built optical extinction setup [9].

92 2.2 Preparation of gold nanoparticles on glass slides and Scanning Electron Microscope (SEM)  
93 measurements

94 Glass slides (Carol Roth & Co. KG, Germany) were cut at the size of about  $25 \times 8 \text{ mm}^2$  with a  
95 diamond tip, washed in a solution of Decon 90 and deionized water (18.2  $\Omega$ ) (2:8, v/v ratio) into an  
96 ultrasonic water bath at 50°C for 15 min according to [10].

97 Commercial TEM copper grids (200 mesh, diameter of 3.05 mm grids)(Strata Tek™ Double  
98 Folding Grids, Ted Pella, Inc.) with double folding were fixed with scotch-tape onto the processed  
99 glass slides for a maximum of 3 double grids located on the same glass slide prior to gold  
100 evaporation, to obtain a pattern of 100 or 200 well per grid. Gold was evaporated by using a MEB  
101 400 (PLASSYS, France) evaporator at the following conditions:  $1.0 \times 10^{-6}$  Torr at 40°C, and an  
102 evaporation rate of 0.08 nm/s to obtain a gold thickness of 4 nm. After evaporation, the TEM masks  
103 were removed and the gold covered glass slides were transferred in an oven (Naberthem, Germany)  
104 at 500 °C for 8 h to allow the formation of the gold nanoparticles (NPs) by thermal annealing before  
105 a washing step with an acetone-ethanol (1:1) mixture in an ultrasonic water bath at 30 °C for 30  
106 min. To verify the gold surface of bare gold nanoparticles and their interspatial distance Scanning  
107 Electron Microscope analysis were made using a field emission scanning electron microscopy  
108 (Raith, SEM-FEG-eLine, France) at the following conditions: accelerating voltage of 10 kV,  
109 working distance of 8.8 mm, samples covered with an ultrathin layer (3 nm) of palladium by  
110 sputter-coating to suppress the charging effect.

111 2.3 DNA probes

112 The specific DNA probe for *B. bruxellensis* (Thiol-Brett-probe)(MWG, GmbH Ebersberg,  
113 Germany) [11, 12] was modified at 5' end by the addition of a thiol group: 5'-ThiC<sub>6</sub>-  
114 TGTTTGAGCGTCATTTTCCTTCTCATHiC<sub>6</sub>TGTTTGAGCGTCATTTTCCTTCTCACTATTTAGT  
115 GGTTATGAGATTACACGAGG -3'.

116 A DNA sequence complementary to the Thiol-labelled probe was used as a positive control. The  
117 Thiol-Brett-probe was used at 100 ng/ $\mu$ L, while the sequence complementary to the capture probe  
118 was standardized at 0.01, 0.1, 1 and 10 ng/ $\mu$ L prior to be used.

#### 119 2.4 Biofunctionalization of gold nanoparticles

120 The immobilization of the DNA probes on the surface of the gold nanoparticles (NPs) was realized  
121 through thiol chemistry. The Thiol-Brett probe (capture probe) was used at 100 ng/ $\mu$ L. Then, 3  $\mu$ L  
122 of the capture probe, previously denatured at 95°C for 5 min, were allowed to bind to the gold  
123 nanoparticles using 1X SSPE buffer at 4°C for 1, 2, and 6 h each, in order to optimize the probe-  
124 NPs hybridization conditions for the biofunctionalization of the glass slides.

#### 125 2.5 Microorganisms and DNA samples analysis

126 Pure yeast strains cultures of *Brettanomyces bruxellensis* DSM70726 (Deutsche Sammlung von  
127 Microorganismen und Zellkulturen GmbH, Braunschweig, Germany) as positive sample, and  
128 *Saccharomyces cerevisiae* DSM70424 as negative sample, were used for testing the specificity and  
129 sensitivity of the biosensor. The yeasts were cultured in Malt Extract broth (Oxoid, Milan, Italy)  
130 and Malt Extract Agar (Oxoid) prior to be used for the experiments. The DNA of the reference  
131 strains was extracted and purified from one millilitre of overnight broth culture using the Wizards  
132 Genomic DNA Purification Kit (Promega, Milan, Italy) [11]. The purity and concentration of the  
133 DNA samples were evaluated by using a Varian Cary 100 UV-Vis spectrophotometer (Agilent  
134 Technologies). DNA samples were standardized using sterile ddwater.

135 LSPR experiments were carried out using 2  $\mu$ L of the DNA sequence complementary to the capture  
136 probe (positive control) at 0.01, 0.1, 1 and 10 ng/ $\mu$ L to optimize the sample-capture probe  
137 hybridization step. Finally, 2  $\mu$ L of the DNA samples from two selected yeasts (*B. bruxellensis* and  
138 *S. cerevisiae*) at 0.01, 0.1, 1 and 10 ng/ $\mu$ L were used to test the specificity and sensitivity of the  
139 LSPR technique. Both the complementary sequence and DNA samples from *B. bruxellensis* and *S.*  
140 *cerevisiae* were added to the biofunctionalized glass slide after denaturation at 95°C for 5 min, and  
141 allowed to hybridize to the capture probe for 2 h at room temperature.

## 142 2.4 LSPR measurements and processing data

143 The LSPR measured the extinction spectrum (absorption + scattering) of the nanoparticles obtained  
144 by recording the intensities of transmitted radiation for the different wavelengths of a white light  
145 source. The wavelength shift and optical density for bio-functionalization steps were compared.  
146 Changes in the optical properties of the nanoparticles due to DNA-probe binding are reflected in the  
147 shift of LSPR extinction maximum ( $\lambda_{\max}$ ). Each different concentration of the DNA was deposited  
148 onto one TEM grid. Specifically, four patterns were chosen for each grid located on the glass slide,  
149 and LSPR measurements on the same patterns after bio-functionalization steps were made. The  
150 resulted LSPR spectra were measured and compared with those ones of clean NPs (NPs with no  
151 linked DNA-probe). SpectraSuite-Spectrometer Operating Software was used to acquire LSPR data  
152 and register the maximum spectra extinction. Furthermore, all the aquired data were processed with  
153 software Origin Pro 8.5.

154

## 155 3. Results and Discussions

### 156 3.1 Optimization of the buffer for LSPR measurements

157 The standard extinction spectrum of bare NPs measured from four patterns /TEM grid, among 3  
158 independent grids, had an average of 552.76 nm with an Optical Density (OD) of 0.2094.  
159 Generally, after each biofunctionalization using the DNA-probe complex of Au NPs, the three  
160 resulted resonant wavelengths had a red shift compared to bare NP's. Thus, the average wavelength  
161 of the DNA samples in the presence of TRIS-HCl was 557.43 nm, of PBS was 566.33 nm and of  
162 SSPE was 574.45 nm, respectively (Table 1). Such results imply a difference of the peak shift when  
163 using gold nanoparticle of 4.67 nm, 13.57 nm and 21.69 nm, for TRIS-HCl, PBS, and SSPE buffer,  
164 respectively. Interestingly, the 1X SSPE buffer showed the highest amplitude peak with 0.3545 OD  
165 and the greatest increase of LSPR spectra, thus it was selected for the subsequent experiments. The  
166 LSPR extinction spectra measured for pure NPs (Au NPs) and biofunctionalized Au NPs using the  
167 TRIS-HCl, PBS and SSPE buffers at the same conditions are reported in Figure 1.

168

### 169 *3.2 SEM characterization*

170 By using Scanning Electron Microscopy (SEM) imaging characterization, it was found that gold  
171 nanoparticles are homogeneous prepared at 500°C. Thus, such gold structured substrates were  
172 chosen for LSPR experiments (Figure 2).

173

### 174 *3.3 Effect of the time and temperature on biofunctionalization*

175 The average wavelength extinction for the bare AuNPs before functionalization was 555.75 nm.  
176 The average wavelength red shift recorded increased accordingly after the capture probe  
177 immobilization onto the AuNPs, (Figure 3). After 1 h the average wavelength was 560.73 nm, while  
178 after 2 h it was 566.50 nm and finally, after 6 h it was 569.23 nm. In other words the shift calculated  
179 from bare NPs was 4.98 nm, 10.75 nm and 13.48 nm respectively (Table 2). On other hand, the OD  
180 values increased from 0.2928 OD for AuNPs to 0.3873 OD after hybridization of the probe after at  
181 6 h. Based on the data reported previously the time selected for the immobilization of the capture  
182 probe was 1 h because it was considered sufficient to obtain a shift that could indicate the binding  
183 of the DNA probe to the NPs.

184

### 185 *3.4 Short complementary sequence*

186 The average wavelength extinction was 554.72 nm and the OD was 0.2597 OD for Au NPs. The  
187 average wavelength extinction for the biofunctionalized glass surface was 557.5 nm, and after short  
188 sequences hybridization at 0.01 ng/μL, 0.1 ng/μL, 1 ng/μL and 10 ng/μL was, 557.93 nm, 558.01  
189 nm, 559.37 nm and 560.89 nm respectively, as reported in Table 3. Slight shifts were obtained for  
190 the short sequences as shown in Figure 4.

191

### 192 *3.5 Specific detection of B. bruxellensis*

193 The average wavelength for bare NPs was 546.00 nm, and 549.87 nm after biofunctionalization.



194 The average wavelength extinction corresponding to the hybridization of *B. bruxellensis* DNA  
195 concentrations of 0.01, 0.1, 1 and 10 ng/μL was 551.23 nm, 553.36 nm, 562.78 nm and 568.27 nm  
196 respectively, as reported in Table 4. The red shift obtained from the described concentrations was  
197 3.87 nm, 5.23 nm, 7.36 nm, 16.78 nm and 22.27 nm, as shown in Figure 5.

198

### 199 3.6 Control experiments using DNA probe from *S. cerevisiae*

200 The average wavelength obtained for *S. cerevisiae* used as negative control was 564.59 nm for the  
201 Au NPs (Optical Density of 0.236), followed by a value of 568.62 nm after biofunctionalization,  
202 and it was 569.57 nm, 568.77 nm, 569.58 nm and 569.23 nm using 0.01, 0.1, 1 and 10 ng/μL DNA  
203 respectively, as reported in Table 5. The red shift obtained for the concentrations was 4.03 nm, 4.98  
204 nm, 4.18 nm, 4.99 nm and 4.64 nm. The value of the extinction was not affected by the DNA  
205 concentrations used, and the red shift was not relevant as shown in Figure 6. The results obtained  
206 using as target microorganism *B. bruxellensis*, and as negative control *S. cerevisiae* demonstrated  
207 the specificity of both the probe and the protocol. Moreover, the washing steps with ddH<sub>2</sub>O, avoid  
208 false signals due to the presence of target DNA not bound to the Au NPs annealed probe, A cut off  
209 value for the extinction wavelength values obtained was defined due to the lack of a proportional  
210 shift wavelength and optical density related to DNA concentrations used during the experiments.  
211 This value allows to distinguish the positive samples from the negative one. The utilization of the  
212 LSPR technique for the detection of the DNA extracted from the wine spoiler yeast allowed to  
213 avoid the utilization of fluorescence molecules in the protocol, and to reduce from two to one the  
214 number of DNA probes commonly utilised. In fact, it was sufficient to modify the 5'-end of the  
215 probe to bind it to the gold surface to obtain a high sensitivity.

216

217

## 218 4. Conclusions

219 An optimized protocol for the LSPR-detection of *B. bruxellensis* onto gold nanostructured  
220 substrates by using a specific Thiol-labelled DNA probe is reported. Moreover, the LSPR  
221 spectrophotometry technique confirmed it is possible to detect 0.01 ng/μL DNA target. A clear  
222 discrimination between the specific hybridization with DNA *B. bruxellensis* and the nonspecific  
223 binding with *S. cerevisiae* DNA was successfully demonstrated using the genomic DNA extracted  
224 from the pure cultures and without the requirement of probe labeling procedures. Due to its high  
225 sensitivity, the LSPR nanobiosensor could be an elegant alternative for the detection of pathogen  
226 microorganisms present in low amount in food and beverage samples.

227

## 228 **Acknowledgements**

229 The authors thank the University of Technology of Troyes for the Stratégique Program 2009–2012  
230 and the Region Champagne-Ardenne grants NANO'MAT for the electronmicroscopy  
231 characterization. Priya Vizzini thanks ERASMUS Programme for funding her stay at the Université  
232 de Technologie de Troyes between 28 of February to 31 of July, 2013. This work was performed in  
233 the context of the COST Action MP1302 Nanospectroscopy.

234

235 **REFERENCES**

236 [1] B. Sepulveda, P.C. Angelomé, L.M. Lechuga, L.M. Liz-Marzà, LSPR-based nanobiosensors.  
237 Nano Today 4 (2009) 244-251.

238

239 [2] A.J. Haes, R.P. Van Duyne, A highly sensitive and selective surface-enhanced nanobiosensor.  
240 Mat. Res. Soc. Symp. Proc. 723 (2002) O3.1.

241

242 [3] L.S. Yung, C.T. Campbell, T.M. Chinowsky, M.N. Mar, S.S. Yee, Quantitative interpretation of  
243 the response of surface plasmon resonance sensors to adsorbed films. Langmuir 14 (1998) 5636-  
244 5648.

245

246 [4] C. Tabor, R. Murali, M. Mahmoud, M.A. El-Sayed, On the use of plasmonic nanoparticle pairs  
247 as a plasmon ruler: the dependence of the near-field dipole plasmon coupling on nanoparticle size  
248 and shape. J. Phys. Chem. A 113 (2009) 1946-1953.

249

250 [5] J. Spadavecchia, A. Barras, J. Lyskawa, P. Woisel, W. Laure, C.-M. Pradier, R. Boukherroub, S.  
251 Szunerits, Approach for plasmonic based DNA sensing: amplification of the wavelength shift and  
252 simultaneous detection of the plasmon modes of gold nanostructure. Anal. Chem. 85 (2013) 3288-  
253 3296.

254 [6] W.K. Jung and K.M. Byun, Fabrication of nanoscale Plasmonic Structures and their  
255 applications, Biomed Eng Lett 1(2011) 153-162.

256

257 [7] I. Abdulhaim, M. Zourob, A. Lakhtakia, Overview of optical biosensing techniques, in: R.S.  
258 Marks, D.C. Cullen, I. Karube, C.R. Lowe, H.H. Weetall (Eds), Handbook of Biosensors and  
259 Biochips, J. Wiley & Sons Ltd, West Sussex, England, 2007, pp. 413-446.

260

- 261 [8] Y. Hong, Y.-M. Huh, D.S. Yoon, J. Yang, Nanobiosensors based on localized Surface Plasmon  
262 Resonance for biomarker detection. *J. Nanomat.* (2012) 1-13.  
263
- 264 [9] K. Jia , J.L. Bijeon, P.M. Adam, R.E. Ionescu, Sensitive Localized Surface Plasmon Resonance  
265 multiplexing Protocols, *Anal. Chem.* 84 (2012) 8020-8027.  
266
- 267 [10] K. Jia, J.L. Bijeon, P.M. Adam, R.E. Ionescu, A facile and cost-effective TEM grid approach  
268 to design gold nano-structured substrates for high throughput plasmonic sensitive detection of  
269 biomolecullest. *Analyst* 138 (2013) 1015-1019.  
270
- 271 [11] F. Cecchini, M. Manzano, Y. Mandaby, E. Perelman and R.S. Marks, Chemiluminescent DNA  
272 optical fiber sensor for *Brettanomyces bruxellensis* detection, *J. Biotechnol.* 157 (2012) 25-30.  
273
- 274 [12] F. Cecchini, L. Iacumin, M. Fontanot, P. Comuzzo, G. Comi, M. Manzano, Dot Blot and PCR  
275 for *Brettanomyces bruxellensis* detection in red wine. *Food Control*, 34 (2013) 40-46.  
276  
277

278 **Table 1: Plasmonic properties (extinction and wavelength) were measured in 4 patterns /grid**  
 279 **for each buffer using gold nanoparticle and the gold NPs annealed to DNA (10 ng/ $\mu$ L) - probe**  
 280 **(100 ng/  $\mu$ L).**

281

Buffer	Resonant wavelength (nm), maximum extinction of the patterns:				Average wavelength extinction	Relative Standard Deviation %	
	1	2	3	4		Wavelength	Extinction
<b>TRIS-HCl</b>	556.27	557.05	557.05	559.37	557.43	0.24	5.31
	0.25	0.22	0.24	0.24	0.24		
<b>PBS</b>	565.56	567.11	564.79	567.88	566.33	0.25	0.46
	0.29	0.29	0.29	0.28	0.29		
<b>SSPE</b>	574.07	575.61	574.84	573.30	574.45	0.17	1.70
	0.34	0.36	0.35	0.36	0.35		

282

283 **Table 2. Plasmonic properties (extinction and wavelength) of the biofunctionalization steps**  
 284 **(hybridization of the probe at 100 ng/  $\mu$ L) to the glass golden surface) were measured in 4**  
 285 **pattern after 1, 2 and 6 h.**

Time	measur e	Resonant wavelength(nm), maximum extinction of the patterns				Average wavelength extinction	Relative Standard Deviation %	
		1	2	3	4		Wavelength	Extinction
<b>1 h</b>	$\lambda$	560.15	562.47	560.15	560.15	560.73	0.20	2.32
	<b>OD</b>	0.32	0.34	0.32	0.32	0.32		
<b>2 h</b>	$\lambda$	567.88	567.11	566.24	564.79	566.50	0.23	2.55
	<b>OD</b>	0.34	0.33	0.33	0.32	0.33		
<b>6 h</b>	$\lambda$	568.66	570.2	570.2	567.88	569.23	0.20	2.38
	<b>OD</b>	0.38	0.39	0.38	0.37	0.38		

286

287

288 **Table 3. Plasmonic properties (extinction and wavelength) of the short sequences (SS)**  
 289 **(sequences complementary to the capture probe) were measured in four patterns after 1, 2**  
 290 **and 3 h hybridization. Capture probe (CP) was used at 100 ng/ $\mu$ L. Values of the short**  
 291 **sequences are expressed in ng/ $\mu$ L.**

292

sample	measure	Resonant wavelength(nm), maximum extinction of the patterns:				Average wavelength extinction	Relative Standard Deviation (RSD%)	
		1	2	3	4		Wavelength	Extinction
CP	$\lambda$	555.5	560.15	560.4	553.95	557.5	0.58	6.62
	OD	0.24	0.28	0.25	0.25	0.25		
SS 0.01	$\lambda$	557.82	557.05	558.6	558.27	557.93	0.12	4.98
	OD	0.29	0.31	0.29	0.28	0.29		
SS 0.1	$\lambda$	556.27	559.37	559.37	557.05	558.01	0.28	7.51
	OD	0.27	0.31	0.32	0.29	0.30		
SS 1	$\lambda$	558.6	559.37	560.15	559.37	559.37	0.11	7.24
	OD	0.27	0.32	0.32	0.31	0.3		
SS 10	$\lambda$	560.15	560.82	560.92	561.69	560.895	0.11	5.82
	OD	0.33	0.29	0.30	0.33	0.31		

293

294

295 **Table 4. Plasmonic properties (extinction and wavelength) are measured in four patterns for**  
 296 **each DNA *B. bruxellensis* concentration used. Values of DNA samples are expressed in ng/ $\mu$ L.**  
 297 **Capture probe (CP) was used at 100 ng/ $\mu$ L.**

298

sample	measure	Resonant wavelength(nm), maximum extinction of the patterns:				Average wavelength extinction	Relative Standard Deviation %	
		1	2	3	4		Wavelength	Extinction
CP	$\lambda$	548.52	550.07	550.07	550.85	549.87	0.17	1.85
	OD	0.18	0.18	0.18	0.18	0.18		
DNA 0,01	$\lambda$	552.4	550.07	552.4	550.07	551.23	0.24	1.22
	OD	0.18	0.18	0.18	0.18	0.18		
DNA 0,1	$\lambda$	553.17	553.95	553.17	553.17	553.36	0.07	6.25
	OD	0.19	0.19	0.21	0.19	0.19		
DNA 1	$\lambda$	563.24	560.15	565.27	562.47	562.78	0.37	8.61
	OD	0.25	0,24	0.22	0.27	0.24		
DNA 10	$\lambda$	567.11	569.43	567.11	569.43	568.27	0.23	2.32
	OD	0.26	0.27	0.26	0.27	0.26		



299 **Table 5. Plasmonic properties (extinction and wavelength) are measured in four pattern for**  
 300 **each *S. cerevisiae* DNA concentration. Values expressed in ng/ $\mu$ L. Capture probe was used at**  
 301 **100 ng/ $\mu$ L.**

302

303

sample	measure	Resonant wavelength(nm), maximum extinction of the patterns:				Average wavelength extinction	Relative Standard Deviation %	
		1	2	3	4		Wavelength	Extinction
CP	$\lambda$	570.75	568.72	567.88	567.13	568.62	0.27	1.67
	OD	0.25	0.25	0.25	0.25	0.25		
DNA 0,01	$\lambda$	570	567.88	568.66	571.75	569.57	0.29	1.80
	OD	0.25	0.25	0.24	0.25	0.25		
DNA 0,1	$\lambda$	568.34	567.88	567.88	570.98	568.77	0.26	4.51
	OD	0.24	0.25	0.25	0.27	0.25		
DNA 1	$\lambda$	568.66	569.43	570.11	570.12	569.58	0.12	0.85
	OD	0.25	0.25	0.25	0.25	0.25		
DNA 10	$\lambda$	571.75	567.54	568.66	569.00	569.23	0.31	3.79
	OD	0.26	0.24	0.25	0.25	0.25		

304

305 **Figure 1. LSPR spectra for bare gold nanoparticle and the gold NPs annealed to DNA (10**  
306 **ng/ $\mu$ L) - probe (100 ng/  $\mu$ L) using SSPE, PBS and Tris-HCl buffer at the same experimental**  
307 **conditions.**

308

309 **Figure 2. Scanning Electron Microscope (SEM images) of bare are gold nanoparticles.**

310

311 **Figure 3. LSPR spectra for immobilized probe at 100 ng/ $\mu$ L after 1, 2 and 6 h. Proportional**  
312 **increase of the redshift wavelength with the time.**

313

314 **Figure 4. LSPR spectra of short sequence complementary to the Thiol - Brett probe (100**  
315 **ng/ $\mu$ L)used at 0.01, 0.1, 1 and 10 ng/ $\mu$ L. A slight wavelength shift caused from the short length**  
316 **of the sequences is present.**

317

318 **Figure 5. *Brettanomyces bruxellensis* LSPR spectra of bare Au NPs, *B. bruxellensis* DNA at**  
319 **0.01, 0.1, 1 and 10 ng/ $\mu$ L. The hybridisation between the gold surface linked DNA Thiol probe**  
320 **and the yeast DNAs was conducted at room temperature for 2 h.**

321

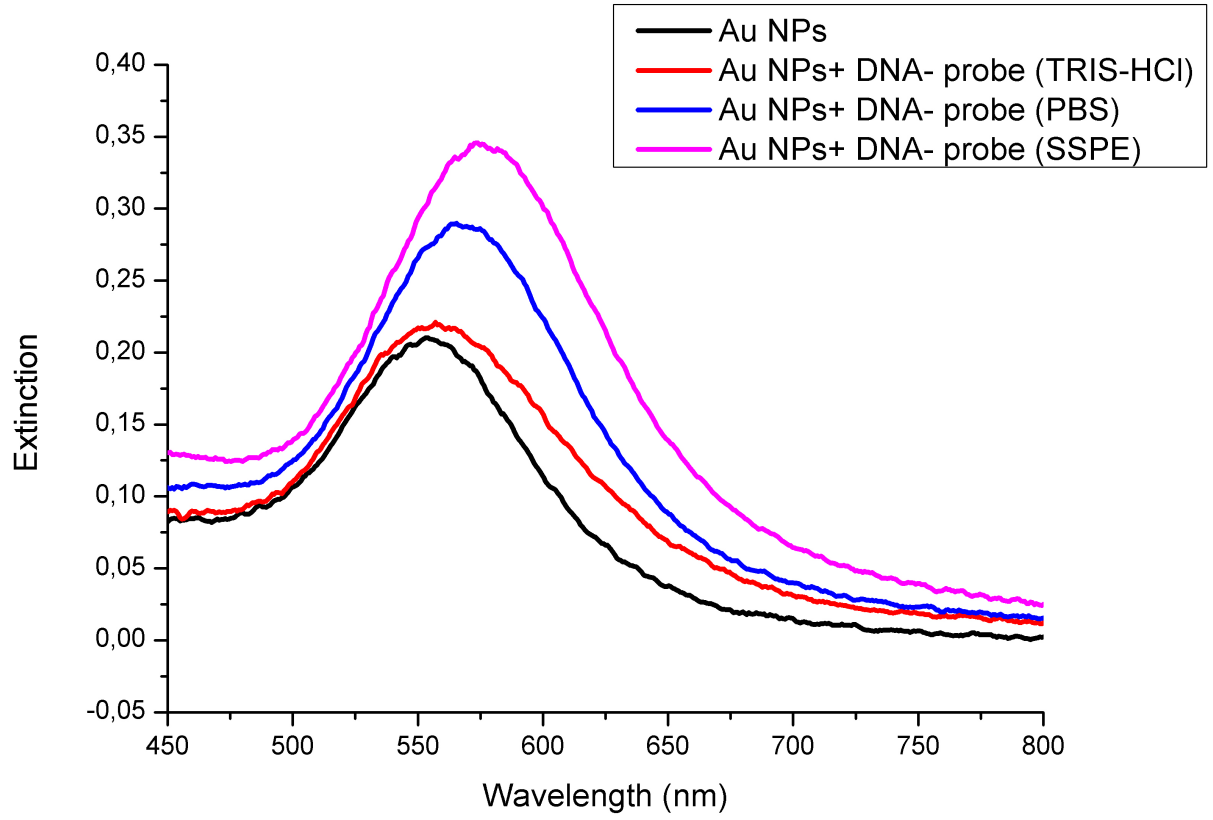
322 **Figure 6. *S. cerevisiae* LSPR spectra of bare Au NPs, *S. cerevisiae* DNA at 0.01, 0.1, 1 and 10**  
323 **ng/ $\mu$ L. The hybridisation between the gold surface linked DNA Thiol probe and the yeast**  
324 **DNAs was conducted at room temperature for 2 h.**

325

326

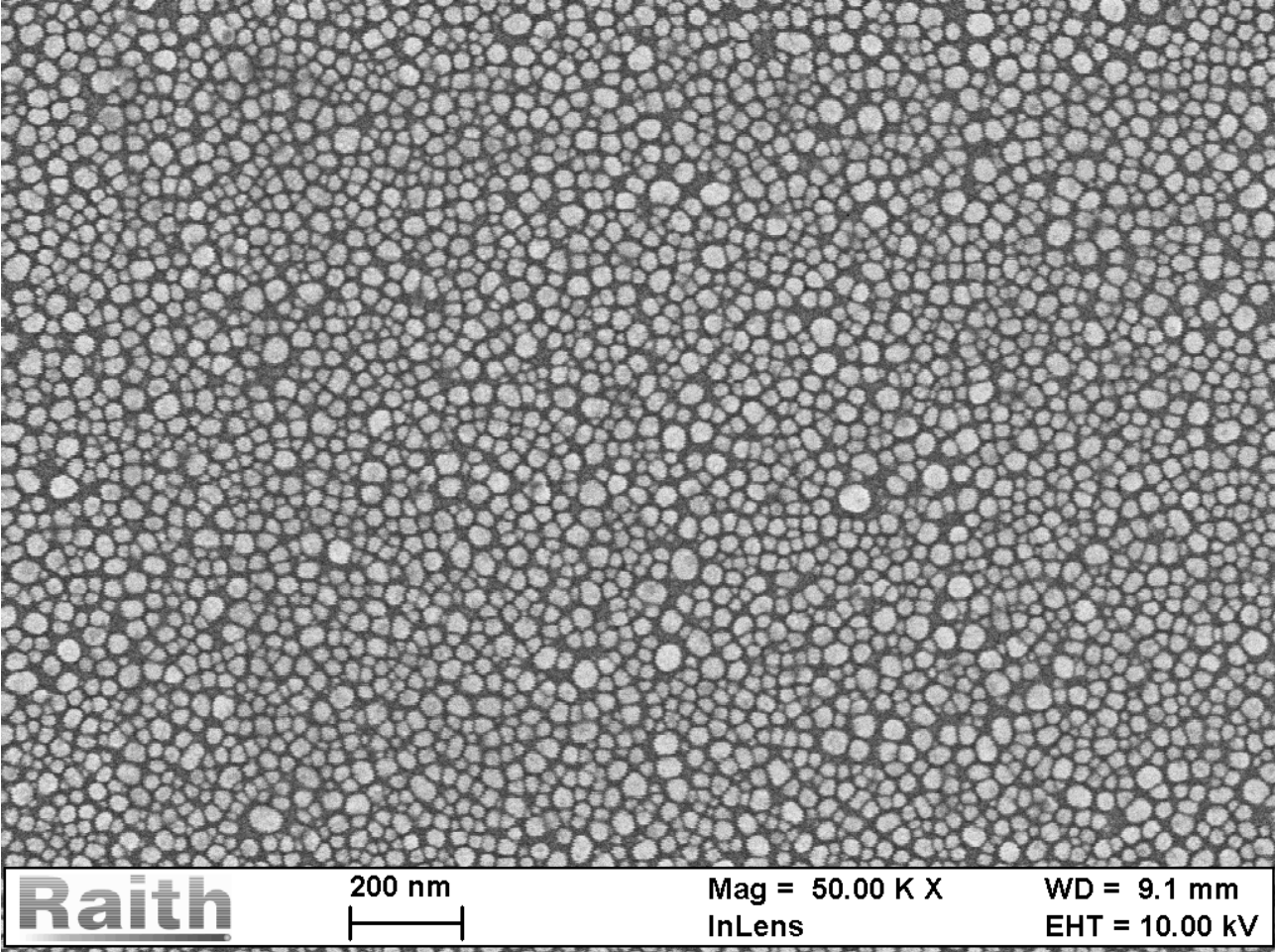
327

328 **Figure 1**



329

330



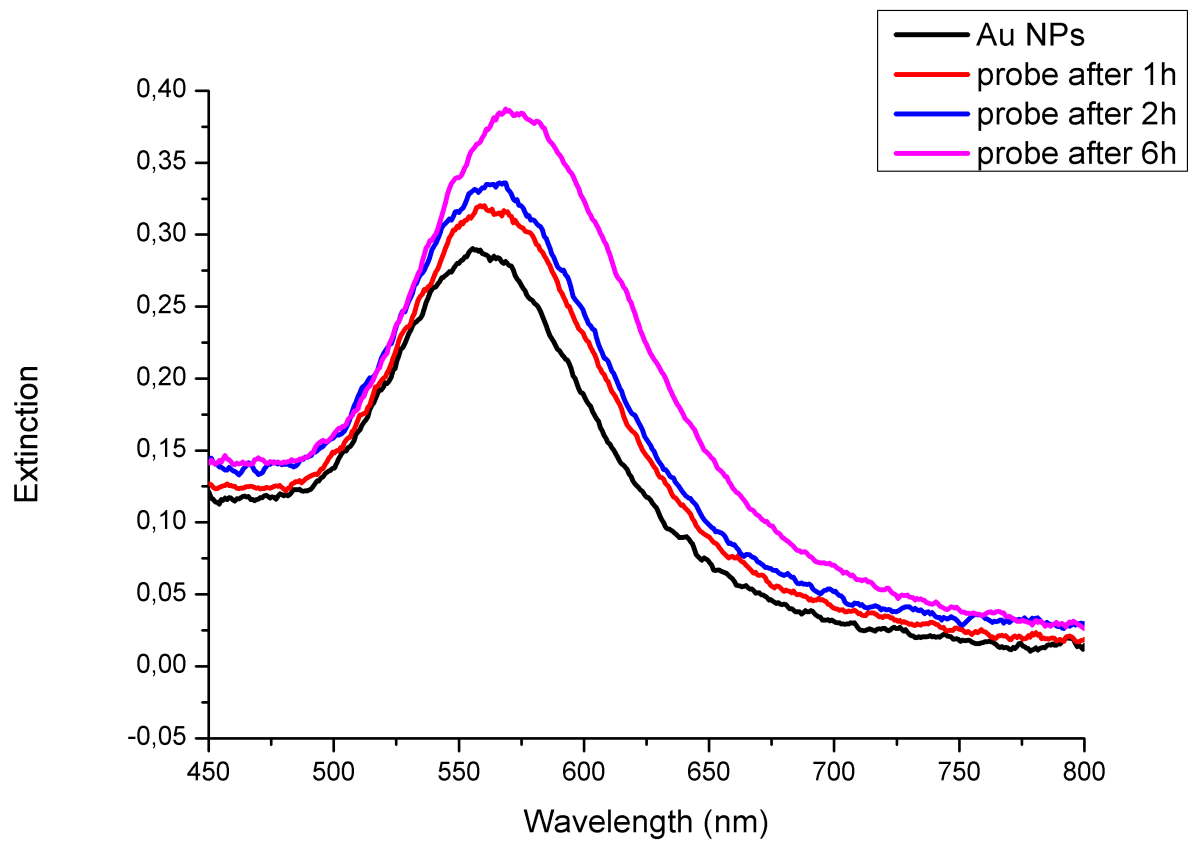
331

332

333 **Figure 2**

334

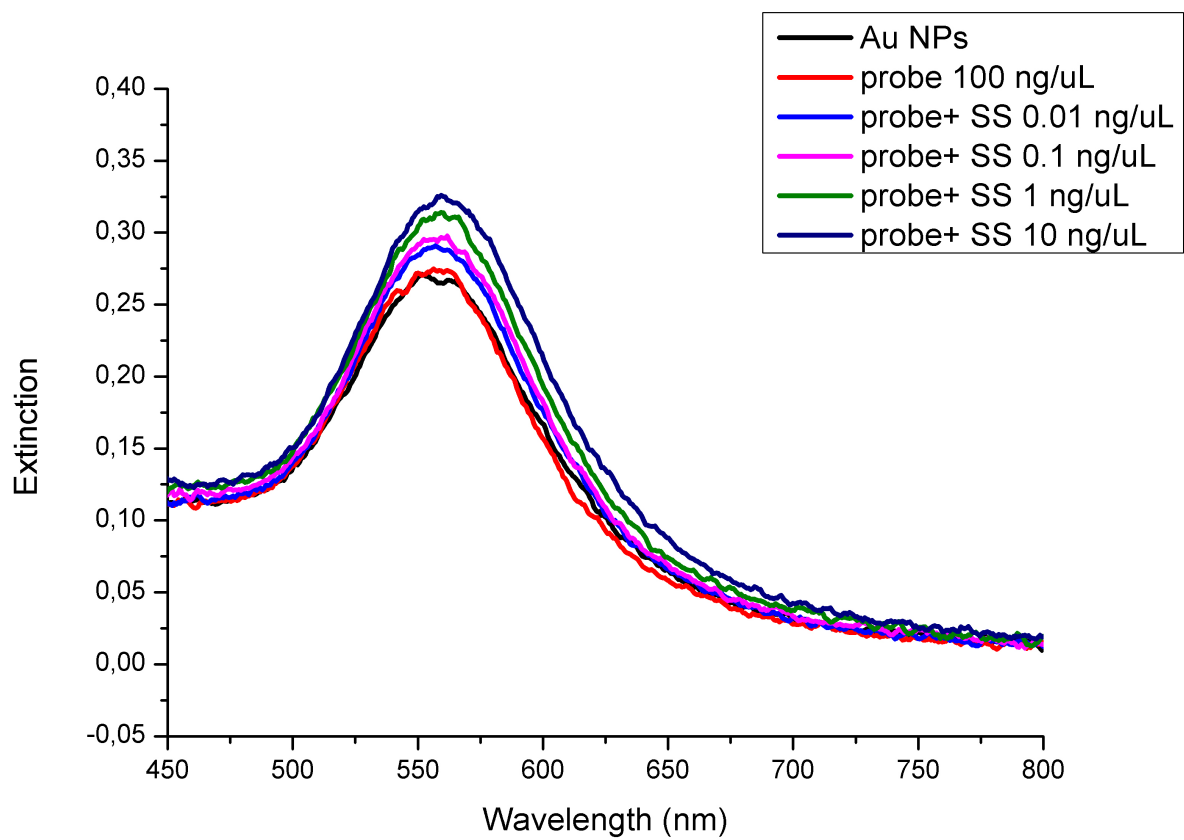
335 **Figure 3**



336

337

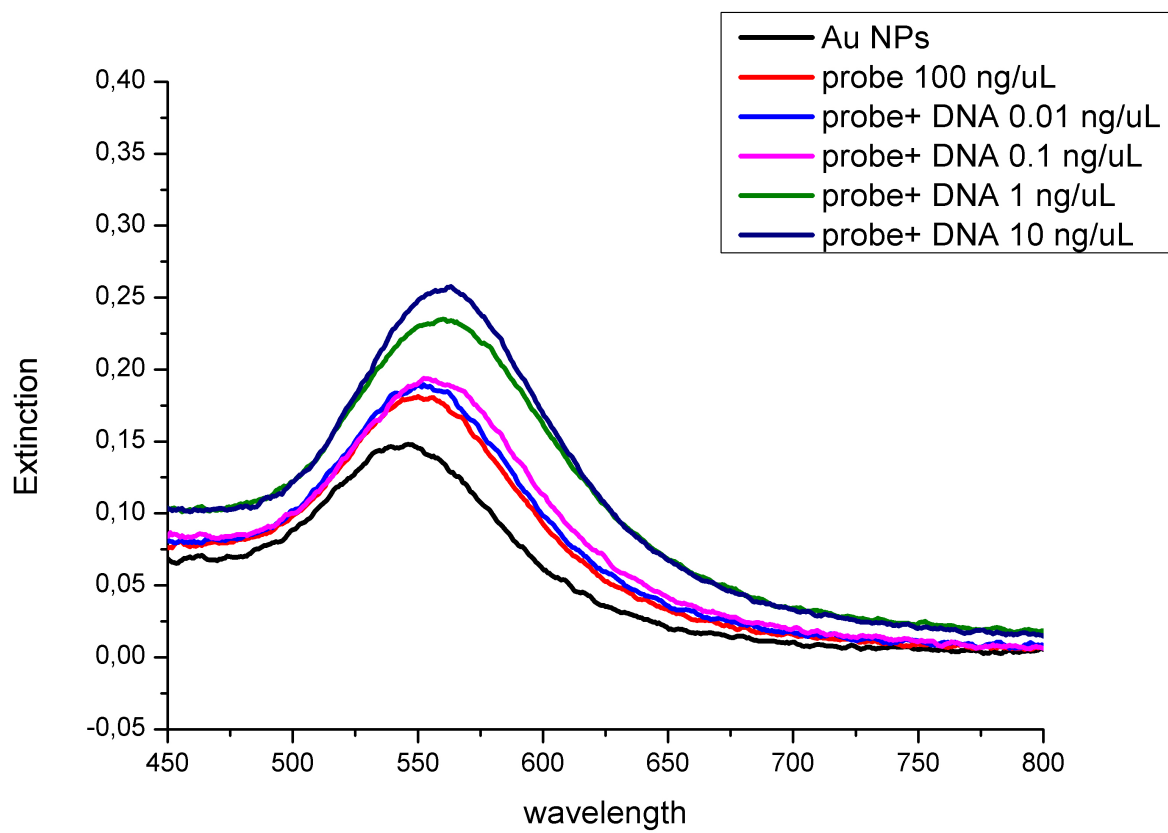
338 **Figure 4**



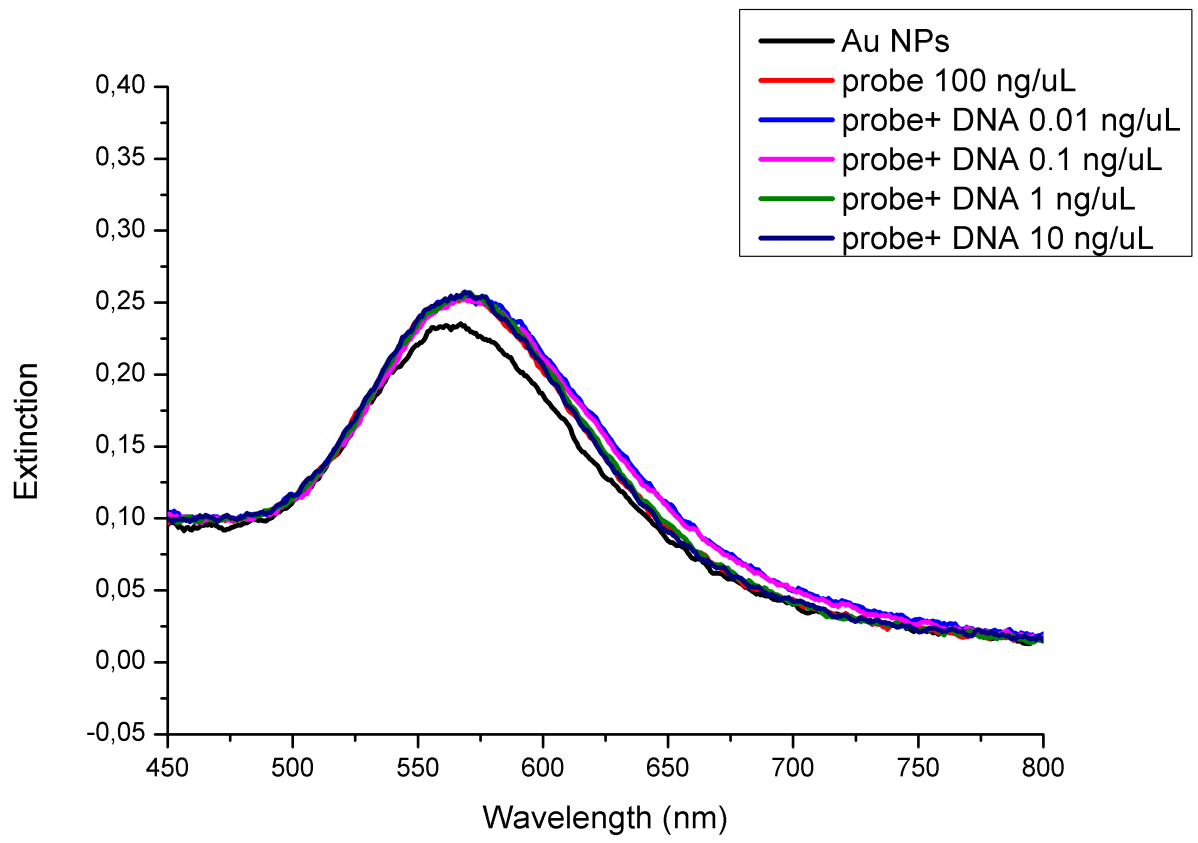
339

340

341 **Figure 5**



342



343

344 **Figure 6**

345